

# Why thermal isomerization of the chromic switch spiropyran-merocyanine is enhanced in polar protic solvents. A computational study of the reaction mechanism.

Olha Kovalenko<sup>†</sup>, Mar Reguero<sup>\*</sup>

Departament de Química Física i Inorgànica, Universitat Rovira i Virgili, c/Marcel·lí Domingo 1, 43007 Tarragona, Spain.  
E-mail: mar.reguero@urv.cat

Received xxxxxx

Accepted for publication xxxxxx

Published xxxxxx

## Abstract

Spiropyran (SP) is a chromic material that undergoes isomerization to merocyanine (MC) under irradiation. To extend its applicability as a molecular switch, it would be convenient to be able to induce and control its isomerization also in the dark, what seems to be possible in acidic media. We present here a computational study of the mechanism of isomerization of protonated SP. We have found that protonation induces the stabilization of MC, protonated at O, relative to SP, protonated at N. Given the different site of protonation for both species, the ring-opening reaction must take place together with a proton transfer event. We have shown that the barrier of this process decreases if a protic solvent molecule takes part in the reaction. In this way, the rate determining step of the process is the isomerization between different rotamers of protonated MC. The detailed knowledge of the reaction mechanism can help in the design of structural or electronic modifications of SP to improve its switchability.

Keywords: Molecular switch; chromic materials; spiropyran; merocyanine; DFT; reaction mechanism.

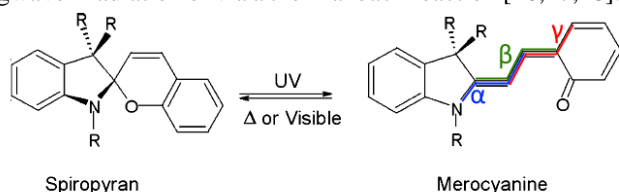
## 1. Introduction

Chromic materials, which undergo induced reversible switching between two stable states or isomers with different physical and chemical properties [1] have been intensively studied in recent years due to their potential application in drug delivery systems [2,3] and sensors [4,5], for optical storage [6,7], or as functional components of molecular electronic devices. In the last case they act as switches, transistors, rectifiers or molecular wires. The possibility of modifying their electronic or geometrical structure in their chemical synthesis [8] allow creating ultraminiaturized

elements of electronic devices with tailored structures and properties [9].

In particular, one of the most interesting and studied chromic materials is spiropyran (SP) [10,11,12]. Some characteristics of SP such as its fatigue resistance, the possibility of modifying its properties by substitution or the capacity of being switched between isomers by irradiation, with high quantum yields, has attracted the interest of scientists and technologists. On top of the mentioned above applications, SPs can also be used as a component of molecular machines [13] or for construction of functional materials incorporating it into polymeric matrices [14] or combining it with carbon nanomaterials [15].

Spiroyrans consist of two heterocycles, benzopyran and indole, which are linked by a  $sp^3$ -hybridized carbon that keeps both moieties perpendicular to each other and prevents conjugation of the two  $\pi$ -electronic systems, resulting in a colourless compound. Under UV irradiation the  $C_{\text{spiro}}-O$  bond undergoes heterolytic cleavage (Scheme 1) that leads to the formation of the open coloured form merocyanine (MC), which absorbs in the visible region due to an extended  $\pi$ -electronic system. MC returns to the original form under longwave irradiation or via a thermal back reaction [16,17,18].



**Scheme 1.** Reversible photoisomerization of SP-MC system.

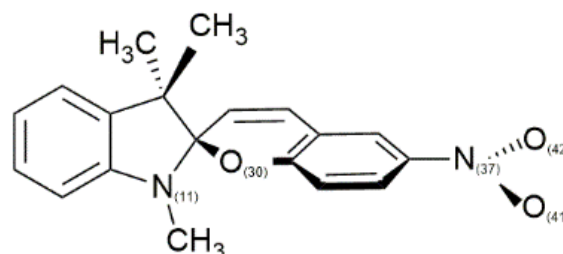
To extend the applicability of SP, it would be convenient to be able to control its isomerization without the need of radiation. In fact, this can be achieved by protonation of the spiroyrans molecule in acidic media [19,20]. This environment induces a proton addition that changes the structure and properties of SP. This protonated form can be useful in the design of some particular molecular devices, for instance, as a component for proton transfer in photoelectric cells [21,22]. But for really being of practical interest, it must be possible to control the rate and yield of the isomerization reaction. Given that irradiation is not expected to be involved in these applications, to obtain a fast response it is necessary to make the thermal isomerization a fast process by decreasing the barrier of its reaction path. To find out how to achieve this, without the long and expensive experimental method of trial and error, it is convenient to know in detail the mechanism of the reaction and analyse the factors (external like the environment or internal like substituents that modify the structure of the reactant) that influence on the reaction.

In this line, some works have already been performed studying the effect of protonation on the isomerization pathway and on the structural properties of SP and MC. Experimental studies [23,24] suggest that protonation on the pyran O at room temperature makes SP unstable and leads to the cleavage of the  $C_{\text{spiro}}-O$  bond, with the subsequent formation of cis-MC. But this reasoning to explain the opening of the spiro ring is not compatible with the hypothesis suggested in many other works, which assume, although with lack of systematic studies, that the most favourable site of protonation of SP is the N atom of the indoline moiety, what stabilizes significantly the SP form [19,21,22,23,25,26,27,28].

Surprisingly, in spite of the previous assumptions, the question of how the proton is transferred from N in SP to O in MC has never been addressed before, although for designing efficient and reliable devices it is crucial to understand all the

processes that the different components of the device can undergo.

In this paper we report a detailed computational study of the thermal isomerization reaction of a protonated SP, 1,3-dihydro-1,3,3-trimethyl-6-nitro-spiro[2H-1-benzopyran-2,2-[2H]indole] shown in Scheme 2, using density functional theory (DFT) computations.



**Scheme 2.** Labelling of the SP derivative studied.

We begin with a study of the thermal ring-opening reaction of neutral SP for comparison purposes, and we report a detailed analysis for the determination of the active sites for protonation, using thermodynamic arguments and Fukui functions. Our results support the previous hypothesis of a preferential protonation in  $N_{(11)}$  (labelling in Scheme 2) for SP and in  $O_{(30)}$  for MC, and consequently we have studied the mechanism of the proton transfer from  $N_{(11)}$  to  $O_{(30)}$ . Our results indicate that the intervention of a water molecule of the solvent environment makes this process kinetically accessible.

## 2. Theoretical background

The determination of the protonation center is an important factor in the elucidation and understanding of the reaction mechanisms involving protonated molecules. The stability of a protonated molecule substantially depends on the site where the proton is attached. The polarizing power of the proton can cause changes in the length and strength of molecular bonds, so the electronic and molecular structures and the energetics of the system can change dramatically upon protonation [29]. It is assumed that changes in energetics and molecular structure will be at its maximum at gas phase.

Protonation reactions proceed via the donor-acceptor mechanism where one of the reagents is a nucleophile and the other one is an electrophile. In our case, spiroyrans proves itself as a nucleophile.

If a molecule has more than one potential site for protonation, the proton attachment can take place at all possible sites for protonation, even if protonation on different sites are non-equiprobable, but in the eventual situation of equilibrium the proton will preferentially be found attached to the most suitable site for protonation. This site can be predicted from comparing energies of all protonated species. It can be also determined from the electron density difference

between neutral and charged molecule in terms of conceptual descriptors, such as the Fukui function, that can be conveniently described in the frame of the Density Functional Theory.

The Fukui function is a local descriptor that indicates the regions of a chemical system where the electron density will preferentially change when the number of the electrons of the species is modified.

Parr and Yang determined the Fukui function,  $f(r)$  [30,31] according to the following formula:

$$f(r) = \left[ \frac{\partial \rho(r)}{\partial N} \right]_{V(r)} \quad (1)$$

where  $\rho(r)$  is the electron density,  $N$  is the number of electrons and  $V$  stands for the external potential (potential of the core-electron attraction plus any other potential that is applied to the system).

The Fukui function (1) characterizes the response of the electron density to the change in the number of electrons with a constant external potential (fixed location of the nuclei).

Parr and Yang suggested associating the derivative in equation (1) with different reactivity indices due to the lack of its continuity (since for systems with a finite number of atoms or molecules, the derivatives of equation (1) on the right and on the left are unequal). Thus, for nucleophilic attack, we have:

$$f(r)^+ = \left[ \frac{\partial \rho(r)}{\partial N} \right]_{V(r)}^+ \quad (2)$$

and for electrophilic attack:

$$f(r)^- = \left[ \frac{\partial \rho(r)}{\partial N} \right]_{V(r)}^- \quad (3)$$

Yang and Parr proposed to use a finite difference scheme to determine  $f(r)$ :

$$f^+(r) \cong \rho_{N+1}(r) - \rho_N(r) \quad (4)$$

$$f^-(r) \cong \rho_N(r) - \rho_{N-1}(r) \quad (5)$$

$$f^0(r) \cong \frac{\rho_{N+1}(r) - \rho_{N-1}(r)}{2} \quad (6)$$

where  $\rho_M(r)$  ( $M=N+1$ ,  $N$  or  $N-1$ ) is the electron density at  $r$  in the  $M$ -electron system. It is important to remember that the integral of the Fukui function over the entire volume of the molecule is equal to unity:

$$\int f(r) dr = 1 \quad (7)$$

Yang and Mortier [32] integrated  $f(r)$  in expressions (4) - (6) over all orbitals of the  $i^{\text{th}}$  atom and obtained quantities that they denoted as condensed Fukui functions  $f_k$  for each  $[k]$  atom in the molecule. The accuracy and adequacy of the values of these condensed Fukui functions depend on the scheme used for the population analysis of the atomic orbitals [30,33]. For a long time, Mulliken's population analysis scheme was the most common, given that it is one of the simplest ones. It has, though, the handicap of being very sensitive to the basis sets [34], reason why nowadays natural bond orbitals (NBO) analysis is the preferred scheme for determination of atomic charges and populations. In fact,

NBO charges are being widely used in calculations of condensed Fukui functions, showing good agreement with experimental results [35].

In this work, condensed Fukui functions calculated based on NBO charges will be used to predict the preferential sites of protonation of SP and MC.

### 3. Methodological procedure

In this study we are going to deal with a medium-sized system to study its ground state reactivity. The size of the system and the extension of the work recommend the use of a not very expensive method. But generally, the contribution of the correlation energy for the transition structures is larger than for the minimum energy structures, so to obtain reliable values of the activation energy it is advisable to use methods that account for the largest part of the electron correlation. Fortunately, in the reactivity of interest there are no excited states involved, so Density Functional Theory (DFT) methods seem to be the most appropriate choice to be used here.

In previous studies for neutral and charged SP-MC systems it was shown that long-range interaction corrected functionals were necessary to describe correctly H bonding. [22] We performed test calculations that showed that the differences between the performance of CAM-B3LYP and PBE0 functionals were not significant so, to be able to compare our results with those published previously, the CAM-B3LYP [36] functional was chosen to be used in this work.

Long range interaction corrected CAM-B3LYP functional [36] that has been used in previous computational investigations of the SP-MC system [22] has been employed here. The basis set 6-31G(d) has been used for geometry optimizations of neutral systems due to its good balance between efficiency and preciseness. For geometry optimization of protonated species, a larger 6-31G(d,p) basis set has been used, given that it contains a p type polarization functions to reduce the effect of the non-uniform electric field arising from the distorted environment of electrons. On the critical points located, single point calculations were performed to recalculate electronic energies, using a cc-pVDZ basis set. Atomic charges were calculated by natural bond orbital (NBO) analysis at CAM-B3LYP/6-31G(d,p) level.

Long range solvent effects were included at the CASSCF/CASPT2 level with the conductor-like version of the polarizable continuum model (C-PCM) [37] where the solvent is treated as an infinite continuum dielectric, while the solute is embedded in a molecular cavity obtained as interlocking spheres centered on each nucleus. The solute cavity was built with the standard United Atom Topological Model, UAH0 procedure, assigning atomic radii on the basis of the chemical connectivity and including the hydrogens in the same spheres as the heavy atoms they are bonded to.

All the calculations have been performed with the Gaussian16 package [38].

## 4. Results and discussion

### 4.1 SP→MC Isomerization pathway for neutral species in gas phase.

Although already known, we have begun this work with the investigation of the SP→MC thermal reaction pathway for the neutral system conversion to have the possibility of comparing the results obtained for the protonated system with those for the neutral one.

As it was shown in previous works [39,40] the process of ring opening of SP involves several MC conformers as intermediates. Merocyanine has eight possible conformers obtained by rotation around the central C-C bonds. These conformers are denoted as CCC, CTC, CCT, TCC, TTT, TCT, CTT, TCC and differ in trans (T) and cis (C) arrangements of the central dihedral angles labeled as  $\alpha$ ,  $\beta$  and  $\gamma$  in Scheme 1. Experimental studies [41,42] have shown that the MC conformers present in solution correspond mainly to TTT and TTC forms.

The structure and coordinates of optimized SP and MC conformers and transition states (TS) linking local minima located in this work are shown in the SI. The character of minima or TS of these structures was checked by frequency calculations, which yielded none (for minima) or one imaginary frequency (for TS) that corresponded to the expected reaction coordinate in each case.

According to our computations, TTC is the most stable conformer, being TTT only slightly less stable (about 1.4 kcal mol<sup>-1</sup>). These results are in a good agreement with previous studies [39,43,44].

The sequence of decreasing stability of all the stable species involved in the reaction studied can be presented as following: SP → TTC → TTT → CTT → CTC → CCC → CCT → TCT. It can be seen, in agreement with previous findings, that conformers with trans configuration for dihedral angle  $\beta$  are more stable than those with cis configuration, what confirms previous findings [45]. TCC conformer was found not to be stable due to the sterical hindrance between pyran oxygen and the methyl groups of the indole moiety.

The critical points located provide the potential energy profile shown in Figure 1.

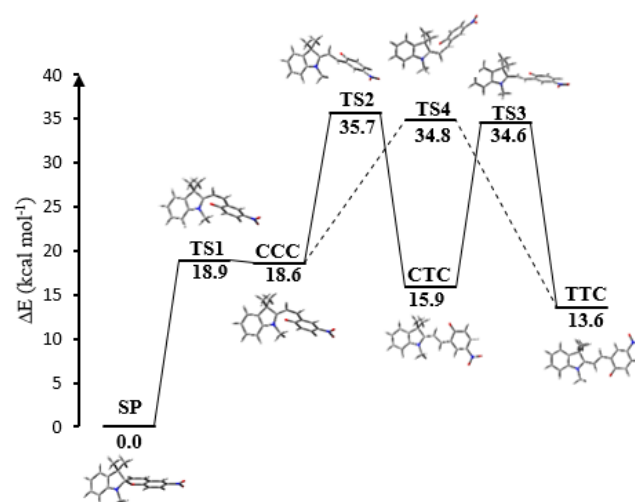


**Figure 1.** Potential energy profile for neutral SP→MC isomerization. Energies (in kcal mol<sup>-1</sup>) relative to spiropyran calculated at CAM-B3LYP/cc-pVDZ level in gas phase.

These results show that, in gas phase, the isomerization begins with the cleavage of the C<sub>spiro</sub>-O bond, but afterwards it takes place stepwise, yielding first the CCC conformer, and evolving from there along different paths depending on the order in which the dihedral angles  $\alpha$  and  $\beta$  change. The energy differences between both paths are not significant, so it can be expected that all minima will be populated as short-lived intermediates of the SP opening reaction.

These results can be compared qualitatively with some computational works on the same system published before. In the one reported in ref. 22, calculations were performed at the CAM-B3LYP/6-311+G(d,p) level and free energies of reaction are reported. For TS1, TS2, TS3 and TS4 the free energies obtained were 16.9 kcal mol<sup>-1</sup>, 28.8 kcal mol<sup>-1</sup>, 27.3 kcal mol<sup>-1</sup> and 28.3 kcal mol<sup>-1</sup> respectively, what conforms a reaction path with lower barriers than the ones reported here. Nevertheless, it must be pointed out that these transition states were not optimized, but located using a grid in two dihedral angles while keeping all other coordinates frozen.

The computations reported in ref. 13 were performed at M06-2X/6-31G(d) level. The results for TS1, TS2 and TS3, 23.2 kcal mol<sup>-1</sup>, 33.8 kcal mol<sup>-1</sup> and 43.1 kcal mol<sup>-1</sup> provide, this time, higher barriers than the one obtained in this work. In any case, the order of magnitude is similar in all cases.

### 4.2 Determination of the preferential protonation centres in Spiropyran and Merocyanine.

A well-known indicator for the electrophilic or nucleophilic centers of a given system is the electrostatic

potential. In our case, the electrophilic positions will be the ones where the proton will preferentially attack.

Figure 2 shows an isodensity surface (0.005) where the electrostatic potential have been mapped in colors, corresponding the red one to the nucleophilic areas and the blue ones to electrophilic ones. The results shows that, in the SP closed form, the heteroatoms  $N_{(11)}$ ,  $O_{\text{spiro}(30)}$ ,  $O_{(41)}$  and  $O_{(42)}$  are all electrophilic, while in the CCC isomer of the MC open form,  $N_{(11)}$  is not electrophilic any longer.

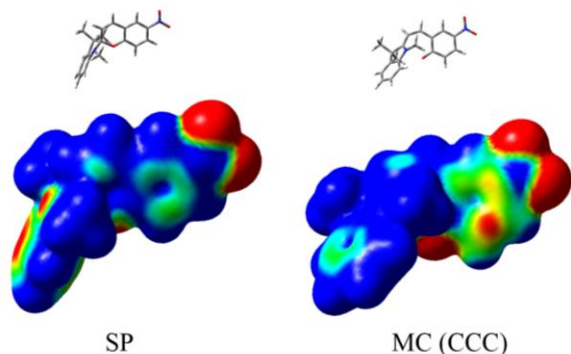


**Figure 2.** Electrostatic potential (from -0.1, in red to +0.1, in blue) mapped on an isodensity surface (of values 0.05) of the closed SP form and of the CCC isomer of the MC open form.

While this is an interesting initial analysis of the problem, it would be convenient to have a quantitative criterion to determine the preferential protonation center. With this aim we have used in this work two different criteria: the thermodynamic one, and the analysis of the local reactivity by means of Fukui functions.

**Thermodynamic criterion.** One of the ways to determine the protonation center is to assume that it will be controlled thermodynamically. In accordance with this approach, we should compare the free energy of all possible protonated species to identify the most stable one. Nevertheless, the entropic factor can be expected to be similar for the species compared (protonated SP in one side and protonated MC on the other), so comparison of energies will similarly give the same qualitative information.

We considered five possible sites of protonation for SP and MC, namely  $N_{(11)}$ ,  $N_{(37)}$ ,  $O_{\text{spiro}(30)}$ ,  $O_{(41)}$  and  $O_{(42)}$  (see Scheme 2), that would give place to the species represented by SP/MC- $N_{(11)}H^+$ , SP/MC- $N_{(37)}H^+$ , SP/MC- $O_{(30)}H^+$ , SP/MC- $O_{(41)}H^+$  and SP/MC- $O_{(42)}H^+$  respectively. Regarding protonated SP species, no minimum was located for SP- $N_{(37)}H^+$ , and optimization of the SP- $O_{(30)}H^+$  gave place to the breaking of the  $C_{\text{spiro}}-O$  bond. This is due to the fact that the arrangement of a proton near pyran  $O_{(30)}$  significantly decreases the electron density of the  $C_{\text{spiro}}-O$  bond that subsequently leads to its cleavage and formation of protonated merocyanine. Keeping the distance of the  $C_{\text{spiro}}-O$  bond constrained, the energy of the optimized SP- $O_{(30)}H^+$  species is very high. On the other hand, protonation on  $N_{(11)}$  of the indole moiety accumulates the

electron density on the  $C_{\text{spiro}}-O$  bond, making of SP- $N_{(11)}H^+$  the most stable SP protonated species. More instable are the species SP- $O_{(41)}H^+$  and SP- $O_{(42)}H^+$ , that present almost the same energy (relative energies are presented in Figure 3).

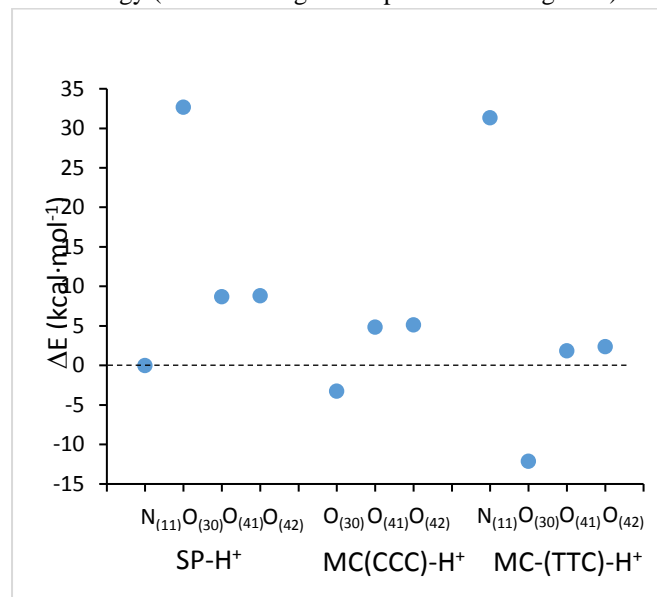


**Figure 3.** Relative energies of different protonated species calculated at CAM-B3LYP/cc-pVDZ level in gas phase ( $E(\text{SP-}N_{(11)}H^+) = -1069.819$  Hartrees).

Regarding protonated MC, we looked for the protonated species expected to be formed immediately after the cleavage of the  $C_{\text{spiro}}-O$  bond, CCC conformations, and those of the most stable conformation of the neutral MC, the TTC isomers. The minimum corresponding to protonation of  $N_{(37)}$  was not found for CCC (so it can be assumed it does not corresponds to a stable specie), and it had a very high relative energy when the MC conformation was TTT. All the other considered protonation centres gave place to stable structures, which relatives energies are shown in Figure 3. The most stable one corresponds to the MC- $O_{(30)}H^+$  isomers, but the species resulting from protonation of CCC-MC shows a value of the dihedral angle  $\alpha$  intermediate between what would correspond to a cis or trans conformation, so we have labelled this species as GCC- $O_{(30)}H^+$  ( $G \equiv$  Gauge). Like for SP, species protonated at  $O_{(41)}$  and  $O_{(42)}$  have similar energies, and they are significantly more stable than the SP species protonated at  $N_{(37)}$ .

These results suggest that for SP protonation takes place at  $N_{(11)}$  but, being MC(GCC)- $O_{(30)}H^+$  more stable than SP- $N_{(11)}H^+$ , the cleavage of the  $C_{\text{spiro}}-O$  bond is a thermodynamically favoured process. An eventual evolution of MC would finally give place to the MC(TTC)- $O_{(30)}H^+$  protonated product.

**Local reactivity criterion using Fukui functions.** Given that the Fukui functions indicate the regions where the electron density will preferentially change (eq. 4-6), they can be used to determine the preferential centers of electrophilic

attack, so we can use it to help to determine the most probable protonation sites for SP and MC. For this reason we calculated the difference of electron density between neutral and cationic species of SP, MC(GCC) and MC(TTC). The results are represented in Figure 4, where the isosurfaces shown correspond to a value of  $|0.007|$  of electron density, representing the green and blue areas those where electron density decreases and increases respectively.

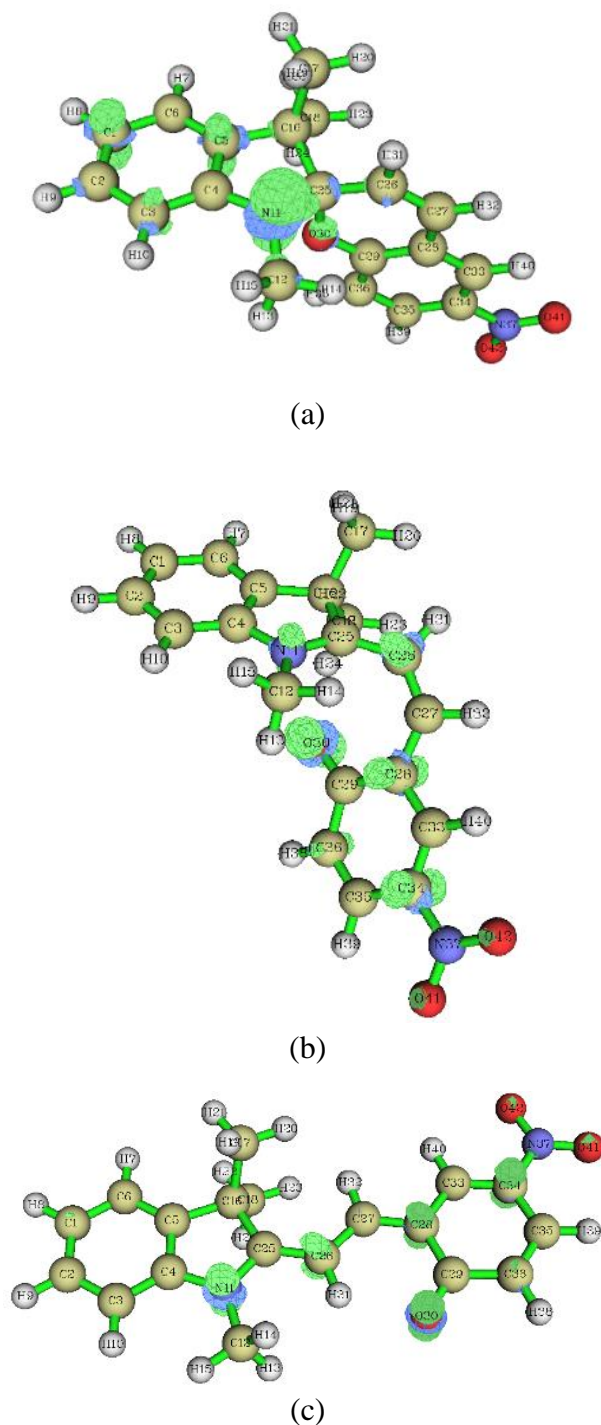


**Figure 4.** Representation of the  $f_k^-(r)$  Fukui function for (a) SP, (b) MC(GCC) and (c) MC(TTC) calculated as the electron density difference between the neutral and cationic species. The isosurfaces correspond to a  $|0.007|$  value of the electron density difference, standing the blue and green areas for negative and positive differences respectively.

Results shown in Figure 4 clearly suggest that in SP,  $N_{(11)}$  is the most and almost only site activated for electrophilic attack, while in MC(GCC) and MC(TTC) there are several possible sites prone to accept protonation.

Given that Fukui functions do not provide a quantitative criterion of the probability of different sites to suffer an electrophilic attack, we obtained the condensed Fukui functions  $f_k^-$ , on the basis of the NBO population analysis, for the most relevant  $k$  sites. The preferential protonation centres will be the ones with maximum values of  $f_k^-$ .

**Table 1.** Values of the condensed Fukui function  $f_k^-$  (for electrophilic attack) computed from NBO charges in gas phase calculated at CAM-B3LYP/6-31g(d,p) level.

Site $k$	$f_k^-$		
	SP	MC(GCC)	MC(TTC)
$N_{(11)}$	0.222	0.042	0.099
$O_{(30)}$	0.003	0.172	0.127
$N_{(37)}$	-0.005	-0.02	-0.017
$O_{(41)}$	0.021	0.063	0.052
$O_{(42)}$	0.023	0.066	0.057

The results given in Table 1 offer a quantitative criterion for the qualitative results shown in Figure 4. In SP, only  $N_{(11)}$  shows a large value of  $f_k^-$ , while in MC(GCC) and MC(TTC) there are several centres with significant values of  $f_k^-$ , although in both cases  $O_{(30)}$  shows a noticeably larger value.

These results corroborate the conclusions derived from the thermodynamic criterion of the previous subsection: while protonation of SP will take place in  $N_{(11)}$ , the most favoured site of protonation of MC isomers is  $O_{(30)}$ . How the proton transfer takes place in the ring opening isomerization of SP to MC and how this transfer affects the isomerization reaction is a question that we will tackle in the next section.

#### 4.3 $SPNH^+ \rightarrow MCOH^+$ pathway of the isomerization reaction in gas phase.

As it was shown above, protonation of the SP molecule will take place at N atom of the indole moiety while all the evidences pointed at the  $O_{(30)}$  as protonation site for MC. Consequently, the isomerization path from protonated SP to protonated MC should begin with  $SP-N_{(11)}H^+$  as initial reactant and include an intramolecular proton transfer event in the ring opening step.

The critical points corresponding to a path similar to the one determined for the neutral system (shown in section 4.1)

were located for the protonated species. They give place to the reaction profile shown in Figure 5. It can be observed that the  $\text{MCH}^+$  species are stabilized relative to the  $\text{SPH}^+$  ones, opposite to the energetics of the neutral system. It indicates that the ring opening reaction is thermodynamically favored for protonated SP.

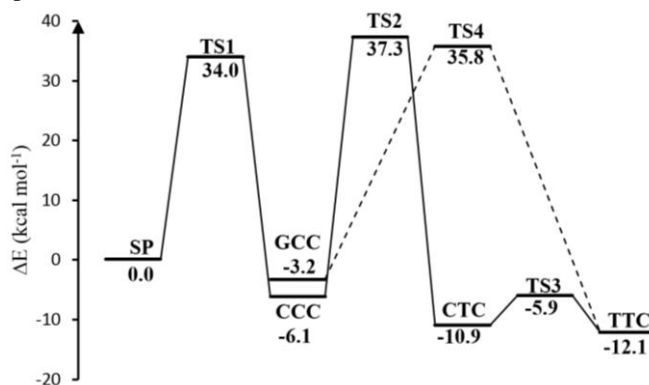


**Figure 5.** Potential energy profile for  $\text{SP-N}_{(11)}\text{H}^+ - \text{MC-O}_{(30)}\text{H}^+$  isomerization. Energies, relative to  $\text{SP-N}_{(11)}\text{H}^+$ , calculated at CAM-B3LYP/cc-pVDZ level in gas phase.

The first step of the mechanism corresponds to a concerted bond-break and proton transfer reaction. Although at the transition state structure the  $\text{C}_{\text{spiro}}\text{-O}$  bond is only slightly stretched (1.550 Å to be compared with 1.392 Å in the  $\text{SP-H}^+$  reactant), the distance between these two atoms increases monotonically as the system evolves, leading to the  $\text{GCC-O}_{(30)}\text{H}^+$  minimum. This result is in agreement with the fact that, according to our calculations, SP protonated at  $\text{O}_{(30)}$  does not exist. All the trials performed in order to find the corresponding  $\text{SP-O}_{(30)}\text{H}^+$  minimum led to open species, indicating that after proton transfer the ring opening process is barrierless. From the  $\text{GCC-O}_{(30)}\text{H}^+$  minimum the  $\text{CCC-O}_{(30)}\text{H}^+$  minimum can also be populated through an very low energy barrier path. From these two minima several isomerization paths to the most stable  $\text{TTC-O}_{(30)}\text{H}^+$  product were found. The most significant ones are represented in Figure 5. One of them corresponds to a direct isomerization from  $\text{GCC-O}_{(30)}\text{H}^+$  to  $\text{TTC-O}_{(30)}\text{H}^+$ , while the other one is an isomerization path that occurs stepwise from the  $\text{CCC-O}_{(30)}\text{H}^+$  minimum through the  $\text{CTC-O}_{(30)}\text{H}^+$  form to the  $\text{TTC-O}_{(30)}\text{H}^+$  product.

According to these results, the overall reaction is exothermic by 12.07 kcal mol<sup>-1</sup>, opposite to the case of the non-protonated system, where it was endothermic by 13.6 kcal mol<sup>-1</sup>. In this case, the reaction proceeds along two or three steps, depending on the isomerization path followed. The two-step path shows slightly lower barriers, but the energy difference is not very significant (37.21 kcal mol<sup>-1</sup> to be compared to 35.81 kcal mol<sup>-1</sup>). Regarding the rate-determining step, our results agree with the previous conclusions derived in ref. 25 from experimental data, that indicated that the rate-determining step is not the ring opening but the subsequent isomerization between  $\text{MC-H}^+$  conformers

(although in that work the proton transfer step was not taken into account). Nevertheless, the difference between the barriers of these steps cannot be considered significant either (34.03 kcal mol<sup>-1</sup> to be compared to 35.81 kcal mol<sup>-1</sup>).

The model used up to here in our computations corresponds to an isolated molecule, so it corresponds, in fact, to the system in gas phase, which can reproduce satisfactorily only non polar solvent environments. To improve our model and be able to analyze the influence of a polar protic solvent, we have to take into account solvent effects, including this environment in the computations.

#### 4.4 $\text{SPNH}^+ \rightarrow \text{MCOH}^+$ isomerization pathway in an acidic aqueous environment.

From the computational point of view, the effects of the solvent can be considered using two different approaches: representing some explicit solvent molecules or considering a polarizable continuum media. In the first case, the model can account for electronic specific interactions between solute and solvent (like hydrogen bonds) while in the second case only the macroscopic properties of the solvent are taken into account. Depending on the solute-solvent couple and on the properties studied, one or the other type of effects will be more or less relevant. Although hydrogen bonds should be included in the first category, the fact that the solvent is described by a distribution of charges that polarizes the electronic structure of the solute, makes that the hydrogen-bond influence on energetics is well described by electrostatic, exchange, and dispersion terms used in continuum models [46]. Consequently, only in the case of solvent molecules playing a role in reaction mechanisms, they will be explicitly included in the description of the model system to be studied in this work.

It is well known the influence that protic solvents like water have in the  $\text{SP-MC}$  equilibrium [47], so the solvent environment should be taken into account when studying computationally this system. In a previous work developed by our group [48] on the photochemical and thermal isomerization reaction of spirooxazine (SO) to MC, we showed that polar solvents change quantitatively the  $\text{SO/MC}$  equilibrium, but the qualitative change is produced by the effect of the hydrogen bonds established when the solvent environment contains protic molecules (like in acetone/water mixtures).

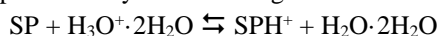
In the case under study here, the effect of specific interactions of protic solvents with the protonated species are expected to be important, mainly in the proton transfer step because, as it will be shown further down, they become a part of the reactive system. On the other hand, this is not the case for the rotational isomerization reaction of MC, and in fact previous studies [24] indicate that the transition state of these

processes are scarcely affected by the presence of water molecules.

According to this, we have studied the ring opening reaction of the protonated system and the isomerization of protonated MC in two different ways. For the ring opening reaction, we have included one explicit water molecule in the system studied at DFT level to account for specific solute-solvent interactions, and have immersed this super-system in a continuum polarizable media by means of the PCM computational approach as implemented in the Gaussian 16 program. On the other hand, for the isomerization of protonated MC, we have only considered the influence of the aqueous environment as a continuum polarizable media.

We have also studied the reaction of protonation of SP to verify the role of this step in the whole reaction. In fact, Wojtik [23] and Hammarson [20] suggested, from experimental studies of the SP/MC isomerization in acidic media, that the equilibrium between the neutral and protonated SP forms play an important role in the ring opening reaction of SP because only the neutral nonprotonated species can undergo the isomerization reaction to MC.

In this work we have included two explicit water molecules in the system to stabilize the  $\text{H}_3\text{O}^+$  moiety when  $\text{H}^+$  is not bonded to SP, so the protonation process studied here can be represented by the following reaction:



The whole profile of the reaction, combining all different phases, is shown in Figure 6. Details of the connection of the profiles of the different phases of the reaction are given in the SI.

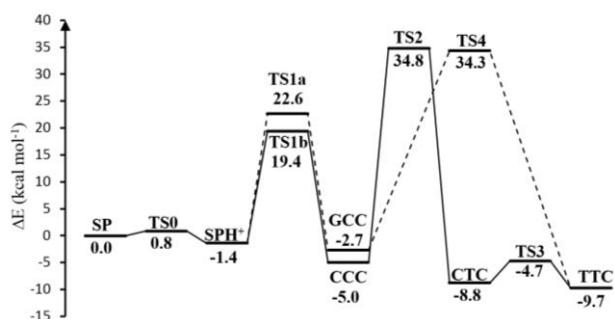


**Figure 6.** Potential energy profile for the protonation and isomerization reaction of SP in acid aqueous media. Energies calculated at CAM-B3LYP/cc-pVDZ level.

Our results for the first part of the reaction (optimized geometries depicted in the SI) showed that the protonation of SP is slightly exothermic by  $1.40 \text{ kcal mol}^{-1}$ . It was not possible to fully optimize the TS of this reaction (TS0 in Figure 6), but partially optimized geometries together with scans along the reaction coordinate allow giving an upper bound for the value of the energetic barrier that is extremely low, of  $0.84 \text{ kcal mol}^{-1}$ . This is in agreement with the conclusions of the study presented in ref. 20 that states that the establishment of the equilibrium between SP and  $\text{SPH}^+$  is extremely fast compared to that between SP and MC.

The next step of the reaction, the concerted ring opening and proton transfer reaction, was found to be also slightly exothermic, like in gas phase, being  $\text{GCCOH}^+$   $3.6 \text{ kcal mol}^{-1}$  more stable than  $\text{SPH}^+$ . Two transition states were found for this reaction, schematically shown in Figure 7. The one shown in panel (a) correspond to a direct migration of the proton in the form of  $\text{H}_3\text{O}^+$ , as expected to be found in an acidic aqueous solution. The barrier of this reaction is  $22.6 \text{ kcal mol}^{-1}$ . The second transition state, shown in panel (b) correspond to a water-mediated proton transfer in such a way that there is a concerted migration of the proton attached to  $\text{N}_{(11)}$  in  $\text{SPH}^+$  to the water molecule and of a proton of the  $\text{H}_3\text{O}^+$  to  $\text{O}_{(30)}$  in  $\text{MCH}^+$ . That is it, there is a substitution of a H atom in the water molecule, so the proton attached to  $\text{N}_{(11)}$  in  $\text{SPH}^+$  is not the same that the one attached to  $\text{O}_{(30)}$  in  $\text{MCH}^+$ . The barrier for this mediated proton transfer is  $3.25 \text{ kcal mol}^{-1}$  lower than the one for the direct migration, what shows the role of the protic solvents in this reaction.

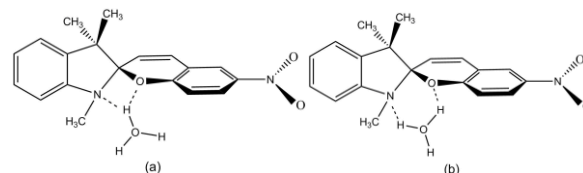


**Figure 7.** Schematic representation of the transition state geometries found for the proton transfer from  $\text{N}_{(11)}$  to  $\text{O}_{(30)}$ : a) direct migration; b) water-assisted migration.

The rate of this reaction step, nevertheless, will be faster than expected in relation with this height of the barrier given that, being the reaction the transfer of a proton, tunnelling effect will accelerate this reaction step.

The profile of the last part of the reaction, the isomerization of protonated MC in an aqueous environment, is very similar to the one in gas phase. Both the stepwise and the direct isomerization paths connecting  $\text{GCCOH}^+$  and  $\text{CCCOH}^+$  with  $\text{TTCOH}^+$  were found in solution, but in this case the barriers of both differ only by  $0.52 \text{ kcal mol}^{-1}$ , so both can be considered effectively equally efficient.

The whole profile shows that the barrier of the proton transfer reaction is, in this case, lower than that of the isomerization step, in agreement with conclusions drawn from experimental observations [24].

Only the results for the isomerization steps can be compared with previous studies. Like in the case of the reaction of the neutral system, we can establish a qualitative comparison with the results given in Ref. 22. The barriers obtained here fit TS2, TS3 and TS4, of  $39.8 \text{ kcal mol}^{-1}$ ,  $4.1 \text{ kcal mol}^{-1}$  and  $36.5 \text{ kcal mol}^{-1}$  (understood as the energy difference between a TS and its immediate previous minimum), can be compared with the free energies of  $30.5 \text{ kcal mol}^{-1}$ ,  $5.0 \text{ kcal mol}^{-1}$  and  $38.9 \text{ kcal mol}^{-1}$  reported in ref. 22.

Scarce quantitative data for barrier energies are obtained from experimental studies. The only one found in the literature (24) reports a cis-MC  $\rightarrow$  trans-MC barrier energy in non-acidic aqueous media of 26.4 kcal mol<sup>-1</sup>, in not very satisfactory agreement with computational results.

#### 4.5 Prediction of the photochromic properties of the protonated system.

The capacity to trigger the isomerization reaction between SP and MC by irradiation in both directions (SP to MC and MC to SP) is an interesting property that this system shows due to the peculiar interplaying between the ground and excited state potential energy surfaces of these isomeric species.

Although the mechanistic study of the excited state reactions is beyond the scope of this work, the comparison between the frontier orbitals of the neutral and protonated species can shed some light in the potential photochromic properties of the later system.

In Figure 8 the frontier orbitals of SP, MC, SPH<sup>+</sup> and MCH<sup>+</sup> are represented.

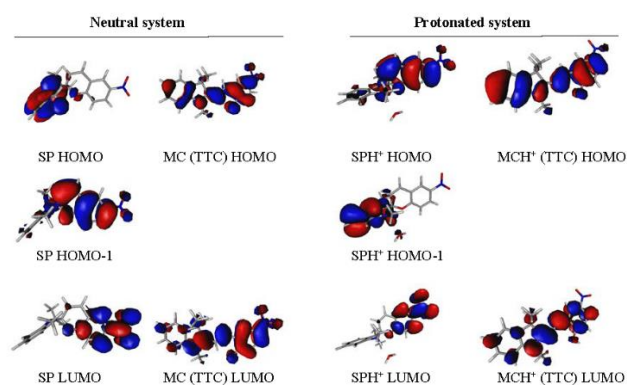


**Figure 8.** Frontier orbitals of the neutral and protonated species.

In the protonated system, like in the neutral one, the frontier orbitals of SPH<sup>+</sup> are located only in one of the two moieties of the molecule, given the orthogonality between the rings prevents the conjugation of the two p-electronic systems. Curiously, HOMO and HOMO-1 are switched in SP and SPH<sup>+</sup>, while LUMOs are similar in both compounds. In spite of the different location of the HOMOs, the absorption of these compounds will continue being in the ultraviolet range, making them colorless.

On the other hand, in MC and MCH<sup>+</sup> both moieties are coplanar, so the conjugation of the p-system expands over the whole molecule. In this case, both HOMO and LUMO are very similar for MC and MCH<sup>+</sup>, indicating that the protic environment will show smaller effects on the MC isomerization reaction and on the chromic properties, yielding

compounds that absorb in the visible region and showing consequently intense coloration.

As a whole, given the similarity of the LUMOs and the equivalence of the HOMOs, it is expected that the chromic and the photochromic properties of the protic system will be the same than those of the neutral one. Nevertheless, this is a hypothesis that should be tested by the corresponding mechanistic study of the excited state reactions.

## 5. Conclusion

In this work we present a systematic study of the mechanism of the isomerization reaction of SP to MC for the protonated system. We have considered the reaction in gas phase and in aqueous media, to understand the role that polar and protic solvents play in the reaction. We have compared these results with those of the reaction of the non-protonated system.

Our results show that the preferential protonation site of SP is N<sub>(11)</sub>, while for MC it is O<sub>(30)</sub>, being this last species (MCH<sup>+</sup>) thermodynamically favored relative to protonated SP (SPH<sup>+</sup>), opposite to the situation for neutral species.

Our mechanistic study shows that the protonation reaction of SP has a very low barrier, so we predict that the equilibrium between SP and SPH<sup>+</sup> species is rapidly established, in agreement with experimental evidences [20,23]. The ring opening reaction can then take place from the neutral SP or from the protonated species SPH<sup>+</sup>. In the second case, the opening reaction must be accompanied by a proton transfer process, from N<sub>(11)</sub> to O<sub>(30)</sub>. We have found a path where these two processes take place concertedly, in gas phase as well as in polar solvents. In the presence of protic solvent molecules (here represented by a water molecule), the lowest barrier path shows that the proton transfer is mediated by a solvent molecule. This alternative lower barrier mechanism explains the substantial changes observed in the SP-MC isomerization reaction in this kind of environments (protic solvents) [24,47].

The barriers obtained for the ring opening process from neutral SP (Figure 1) and from the protonated species in a polar protic solvent (Figure 6) are of the same order, indicating that the isomerization to MC can take place simultaneously from the neutral or protonated forms of SP. Nevertheless, equilibrium in the first case will be almost complete displaced towards SP given that SP is 18.6 kcal mol<sup>-1</sup> more stable than CCC-MC, while in the protonated case the open species will be favored given that CCC-MCH<sup>+</sup> (and GCC-MCH<sup>+</sup>) is more stable than SPH<sup>+</sup> by 2.68 (4.99) kcal mol<sup>-1</sup>. Our results suggest, consequently, that the ring opening reaction will proceed preferentially between protonated species. This conclusion does not agree with the hypothesis presented in ref. 20, which suggests that "MCH<sup>+</sup> is formed via thermal opening SP  $\rightarrow$  MC followed by protonation of MC". This hypothesis is based on the observation that the rate constant of SP isomerization is virtually pH independent, but this fact is also

in agreement with the mechanistic hypothesis presented here, given that both  $SP \rightarrow MC$  and  $SPH^+ \rightarrow MCH^+$  reactions have virtually the same energetic barrier.

The relative energies between rotamers of the neutral and protonated species are similar (-2.7 and -2.3 for  $CCC-MC \rightarrow CTC-MC$  and  $CTC-MC \rightarrow TTC-MC$ , and -3.8 and -0.9 for  $CCC-MCH^+ \rightarrow GTC-MCH^+$  and  $GTC-MCH^+ \rightarrow TTC-MCH^+$ ), but the rotational barriers between species are much lower for the neutral species than for the protonated ones (18.9 for MC and 39.8 for  $MCH^+$ ). Curiously, relative to the initial SP species, the barriers are very similar, around 35 kcal mol<sup>-1</sup>.

These are in the case of  $MCH^+$ , in agreement with the suggestion of ref. 24. Due to the fast energy dispersion to the solvent, the isomerization steps with high barriers will be slow, so for protonated MC, the CCC  $MCH^+$  species must have a significantly long life so it could be possibly detected in solution. This will not be the case of CTC  $MCH^+$ , which will rapidly isomerize to TTC  $MCH^+$  due to the low barrier of this step.

To quantitatively predict the increase of the rate of the isomerization reaction when SP is surrounded by an acidic media, a kinetic study should be performed, but this is beyond the scope of this work. Nevertheless, the reaction profiles provide enough information to explain qualitatively the changes that are expected to be observed in the reaction rates when the system is placed in a protic environment.

The  $SP \rightarrow MC$  reaction for the neutral system is not thermodynamically favored, so it will not take place thermally and must be produced photochemically. On the other hand, once the MC species is obtained (photochemically), the backward reaction  $MC \rightarrow SP$ , although thermodynamically favored, will be a slow reaction when produced in the dark given that its profile presents high barriers. This fact has been extensively observed in previous studies [16-18].

Regarding the reaction in an acidic media, given the extremely fast equilibrium established between the neutral and the protonated forms of SP, the two species will coexist. But while SP will not spontaneously undergo the ring opening reaction,  $SPH^+$  will tend to yield CCC- $MCH^+$  given that this last species is thermodynamically favored. The barrier calculated for the ring opening step can be overcome thermally, but it is high enough to preclude, in principle, a fast reaction. Nevertheless, we must not forget that this step involves a proton transfer, reason why quantum mechanical tunneling effects will be noticeable making this process faster than expected in view of the height of the barrier. Consequently, we can predict a moderately fast reaction to produce protonated MC. But the isomer so obtained will be the CCC one, which is not the most stable one. The barriers of the rotational processes necessary to give the most stable TTC- $MCH^+$  isomer are much higher. Consequently obtaining this last isomer will be, in the best scenario, a much slower process. In fact, the experimental observations of ref. 24

suggest that the rate determining steps of the reaction are the rotational ones, while the experimental work of ref. 19 indicates that the  $MCH^+$  isomer obtained in acidic media is the cis one, while the trans is only obtained after UV irradiation. These observations support our results and the qualitative kinetic predictions derived from them.

As a whole, given that the analysis of the frontier molecular orbitals indicate that the cis  $MCH^+$  species will show the same chromic properties than neutral MC, it is expected that the isomerization reaction of the SP/MC system in an acidic media will be enhanced, while keeping the same chromic properties than in a non-protic environment.

The gained detailed knowledge of the reaction mechanism of this molecular system can help in the design of more efficient molecular switches. The effect of environmental factors such as a protic media on the different steps of the reaction indicates that, if the desired product is the most stable MC isomer, the modifications on the system should be directed to decrease the MC isomerization barriers given that these are the rate determining steps.

### Supporting Information

Test calculations to analyze the effect of different functional groups on the results. Details of the construction of the profile shown in Figure 6; geometries of the minima and transition state structures of the  $SP \rightarrow MC$  Isomerization pathway for neutral species in gas phase; Geometries of the minima and transition state structures of the SP protonation reaction in acidic media; Cartesian coordinates of the critical structures of the reaction mechanisms for the neutral system, for the protonated system in gas phase and for the protonated system in acidic media.

### Author information

Corresponding Author

\*E-Mail: mar.reguero@urv.cat

ORCID

Mar Reguero: 0000-0001-9668-8265

Olha A. Kovalenko: 0000-0002-3153-086X

### Present Addresses

†Department of Electronics, General and Applied Physics, Sumy State University, 2 Rimsky-Korsakov Street, Sumy 40007, Ukraine

### Author Contributions

The manuscript was written through contributions of all authors. All authors have given approval to the final version of the manuscript.

### Funding Sources

Financial support has been provided by the Spanish Administration (Project CTQ2017-83566-P) and the Generalitat de Catalunya (Project 2017SGR629). O. A. K. has received financial support through an EMINENCE II grant, framed in the Erasmus Mundus Action II (European Commission).

**Acknowledgments**

The authors: Olha Kovalenko, Mar Reguero declare that there is no conflict of interests regarding the publication of this paper.

Authors thank Spanish Administration (Project CTQ2017-83566-P) and the Generalitat de Catalunya (Project 2017SGR629) for the financial support. O. A. K. also thanks the European Commission for the Erasmus Mundus scholarship within the framework of the EMINENCE II project".

We thank Yuri M. Lopatkin for drawing our attention to the interest of the study of the isomerization of protonated spipopyran.

**Abbreviations**

SP, spipopyran; MC, merocyanine.

## References

- 1 Tian H., Yang S. Recent progresses on diarylethene based photochromic switches. *Chem. Soc. Rev.* 2004, 33, 85-97.
- 2 Alvarez-Lorenzo C., Bromberg L., Concheiro A. Light-sensitive intelligent drug delivery systems. *Photochem. Photobiol.* 2009, 85, 848-860.
- 3 Barman, S.; Das, J.; Biswas, S.; Maiti, T. K.; Singh, N. D. P. A Spiropyran-Coumarin Platform: An Environment Sensitive Photoresponsive Drug Delivery System for Efficient Cancer Therapy. *J. Mater. Chem. B*, 2017, 5, 3940-3944.
- 4 Shiraishi, Y.; Adachi, K.; Itoh, M.; Hirai, T. Spiropyran as a Selective, Sensitive, and Reproducible Cyanide Anion Receptor. *Org. Lett.* 2009, 11, 3482-3485.
- 5 Ren, J.; Tian, H. Thermally Stable Merocyanine Form of Photochromic Spiropyran with Aluminum Ion as a Reversible Photo-driven Sensor in Aqueous Solution. *Sensors* 2007 7, 3166-3178.
- 6 Ivashenko, O., van Herpt, J. T.; Feringa, B. L.; Rudolf, P.; Browne, W. R. Electrochemical Write and Read Functionality through Oxidative Dimerization of Spiropyran Self-Assembled Monolayers on Gold. *J. Phys. Chem. C* 2013, 117, 18567-18577.
- 7 Willner, I. Photoswitchable Biomaterials: En Route to Optobioelectronic Systems. *Acc. Chem. Res.* 1997, 30, 347-356.
- 8 Małachowski, M.; J.; Żmija, J. Organic field-effect transistors. *Opto-electronics Rev.* 2010, 18, 121-136.
- 9 Kathan, M.; Hecht, S. Photoswitchable Molecules as Key Ingredients to Drive Systems Away from the Global Thermodynamic Minimum. *Chem. Soc. Rev.* 2017, 46, 5536-5550.
- 10 Tamai, N.; Miyasaka, H. Ultrafast Dynamics of Photochromic Systems. *Chem. Rev.* 2000, 100, 1875-1890.
- 11 Samanta, S.; Locklin, J. Formation of photochromic spiropyran polymer brushes via surface-initiated, ring-opening metathesis polymerization: reversible photocontrol of wetting behavior and solvent dependent morphology changes. *Langmuir* 2008, 24, 9558-9565.
- 12 Kovalenko, O.; Lopatkin, Yu.; Konfratenko, P.; Belous, D. Merocyanine-spiropyran relaxation processes. *Eur. Phys. J. D.* 2018, 72: 20
- 13 Wang, P.-X.; Bai, F.-Q.; Zhang, Z.-X.; Wang, Y.-P.; Wang, J.; Zhang, H.-X.; The theoretical study of substituent and charge effects in the conformational transformation process of molecular mechine unit spiropyran. *Org. Electron.* 2017, 45, 33-41.
- 14 Kim, D; Kim, J; Lee T.S. Photoswitchable chromic behavior of conjugated polymer films for reversible patterning and construction of a logic gate. *Polym. Chem.*, 2017,8, 5539-5545
- 15 Zhang, X. Y.; Hou, L. L.; Samorì, P. Coupling carbon nanomaterials with photochromic molecules for the generation of optically responsive materials. *Nat. Commun.* 2016, 7, 11118.
- 16 Berkovic, G.; Krongauz, V.; Weiss, V.; Spiroprans and Spirooxazines for Memories and Switches. *Chem.Rev.* 2000, 100, 1741-1754.
- 17 Mele, E.; Pisignano, D.; Varda, M.; Farsari, M.; Filippidis, G.; Fotakis, C.; Athanassiou, A.; Cingolani, R. Smart photochromic gratings with switchable wettability realized by green-light interferometry. *Appl. Phys. Lett.* 2006, 88, 203124.
- 18 Stitzel, S.; Byrne, R.; Diamond, D. LED switching of spiropyran-doped polymer films. *J. Mater. Sci.* 2006 41, 5841-5844.
- 19 Shiozaki, H. Molecular orbital calculations for acid induced ring opening reaction of spiropyran. *Dyes Pigments* 1997 33, 229-237.
- 20 Hammarson, M.; Nilsson, J. R.; Li, S.; Beke-Somfai, T.; Andréasson, J. Characterization of the Thermal and Photoinduced Reactions of Photochromic Spiroprans in Aqueous Solution. *J. Phys. Chem. B* 2013 117, 13561 - 13571.
- 21 Singh, R.; Böhmb, M. C.; Balasubramanian, G. Energetic and structural properties of different conformations of merocyanine and its protonated forms. *Chem. Phys. Lett.* 2015 633, 287-291.
- 22 Ganesan, R.; Remacle, F. Stabilization of merocyanine by protonation, charge, and external electric fields and effects on the isomerization of spiropyran: a computational study. *Theor. Chem. Acc.* 2012 131, 1255.
- 23 Wojtyk, J. T. C.; Wasey, A.; Xiao, N. N.; Kazmaier, P. M.; Hoz, S.; Yu, C.; Lemieux, R. P.; Buncel, E. Elucidating the mechanisms of acidochromic spiropyran-merocyanine interconversion. *J. Phys. Chem. A* 2007 111, 2511-2516.
- 24 Shiraishi, Y.; Itoh, M.; Hirai, T. Thermal isomerization of spiropyran to merocyanine in aqueous media and its application to colorimetric temperature indication. *Phys. Chem. Chem. Phys.* 2010, 12, 13737-13745.
- 25 Fissi, A.; Pieroni, O.; Angelini, N.; Lenci, F. Photoresponsive Polypeptides. *Photochromic and Conformational. Macromolecules* 1999, 32, 7116-7121.
- 26 Giordani, S.; Cejas, M. A.; Raymo, F. M. Photoinduced proton exchange between molecular switches. *Tetrahedron* 2004, 60, 10973-10981.
- 27 Markworth, P. B.; Adamson, B. D.; Coughlan, N. J. A.; Goerigk, L.; Bieske, E. J. Photoisomerization Action Spectroscopy: Flicking the Protonated Merocyanine-Spiropyran Switch in the Gas Phase. *Phys. Chem. Chem. Phys.* 2015, 17, no. 39, pp. 25676-25688, 2015.
- 28 Klajn R., "Spiropyran-based dynamic materials," *Chem. Soc. Rev.* 2014 43, 148-184.
- 29 Bouchoux, G. Gas-phase basicities of polyfunctional molecules. Part 1: Theory and methods. *Mass. Spectrom. Rev.* 2007, 26, 775-835.
- 30 Arulmoz, S.; Kolandaivel, P. Condensed Fukui function: dependency on atomic charges. *Mol. Phys.* 1997, 90, 55-62.
- 31 Parr, R.G.; Yang, W. Density Functional Approach to the Frontier-Electron Theory of Chemical Reactivity. *J. Am. Chem. Soc.* 1984, 106, 4049-4050.
- 32 Yang, W.; Mortier, W. J. The Use of Global and Local Molecular Parameters for the Analysis of the Gas-Phase Basicity of Amines. *J. Am. Chem. Soc.* 1986, 108, 5708-5711.
- 33 Cioslowski, J.; Martinov, M.; Mixon, S. T. Atomic Fukui indexes from the topological theory of atoms in molecules applied to Hartree-Fock and correlated electron densities. *J. Phys. Chem.* 1993, 97, 10948-10951.
- 34 Jensen, F. Introduction to Computational Chemistry, 2nd edition, John Wiley & Sons: Chichester, UK, 2007.

- 35 Mendoza-Huizar, L.H.; Rios-Reyes, C.H. Chemical Reactivity of Atrazine Employing the Fukui Function, *J. Mex. Chem. Soc.* 2011, 55, 142-147.
- 36 Yanai, T.; Tew, D. P.; Handy, N. C. A new hybrid exchange–correlation functional using the Coulomb-attenuating method (CAM-B3LYP). *Chem. Phys. Lett.* 2004, 393, 51-57.
- 37 Cossi, M.; Rega, N.; Scalmani, G.; Barone, V. Energies, structures, and electronic properties of molecules in solution with the C-PCM solvation model. *J. Comput. Chem.* 2003, 24, 669.
- 38 Gaussian 16, Revision A.03, M. J. Frisch, G. W. Trucks, H. B. Schlegel, G. E. Scuseria, M. A. Robb, J. R. Cheeseman, G. Scalmani, V. Barone, G. A. Petersson, H. Nakatsuji, X. Li, M. Caricato, A. V. Marenich, J. Bloino, B. G. Janesko, R. Gomperts, B. Mennucci, H. P. Hratchian, J. V. Ortiz, A. F. Izmaylov, J. L. Sonnenberg, D. Williams-Young, F. Ding, F. Lipparini, F. Egidi, J. Goings, B. Peng, A. Petrone, T. Henderson, D. Ranasinghe, V. G. Zakrzewski, J. Gao, N. Rega, G. Zheng, W. Liang, M. Hada, M. Ehara, K. Toyota, R. Fukuda, J. Hasegawa, M. Ishida, T. Nakajima, Y. Honda, O. Kitao, H. Nakai, T. Vreven, K. Throssell, J. A. Montgomery, Jr., J. E. Peralta, F. Ogliaro, M. J. Bearpark, J. J. Heyd, E. N. Brothers, K. N. Kudin, V. N. Staroverov, T. A. Keith, R. Kobayashi, J. Normand, K. Raghavachari, A. P. Rendell, J. C. Burant, S. S. Iyengar, J. Tomasi, M. Cossi, J. M. Millam, M. Klene, C. Adamo, R. Cammi, J. W. Ochterski, R. L. Martin, K. Morokuma, O. Farkas, J. B. Foresman, and D. J. Fox, Gaussian, Inc., Wallingford CT, 2016.
- 39 Gómez, I.; Reguero, M.; Robb, M. A. Efficient Photochemical Merocyanine-to-Spiropyran Ring Closure Mechanism through an Extended Conical Intersection Seam. A Model CASSCF/CASPT2 Study. *J. Phys. Chem. A* 2006, 110, 3986-3991.
- 40 Liu, F.; Morokuma, K. Multiple pathways for the primary step of the spiropyran photochromic reaction: a CASPT2//CASSCF study. *J. Am. Chem. Soc.* 2013, 135, 10693–10702.
- 41 Bahr, J. L.; Kodis, G.; de la Garza, L.; Lin, S.; Moore, A. L.; Moore, T. A.; Gust, D. Photoswitched Singlet Energy Transfer in a Porphyrin–Spiropyran Dyad. *J. Am. Chem. Soc.* 2001, 123, 7124-7133.
- 42 Hobley, J.; Malatesta, V.; Giroladini, W.; Stringo, W.  $\pi$ -Cloud and non-bonding or H-bond connectivities in photochromic spiropyrans and their merocyanines sensed by  $^{13}\text{C}$  deuterium isotope shifts. *Phys. Chem. Chem. Phys.* 2000, 2, 53-56.
- 43 Wohl, C. J.; Kuciauskas, D. Excited-state dynamics of spiropyran-derived merocyanine isomers. *J. Phys. Chem. B* 2005, 109, 22186–22191.
- 44 Buback, J.; Nuernberger, P.; Kullmann, M.; Langhojer, F.; Schmidt, R.; Würthner, F.; Brixner, T. Ring-Closure and Isomerization Capabilities of Spiropyran-Derived Merocyanine Isomers. *J. Phys. Chem. A*, 2011, 115, 3924–3935.
- 45 Futami, Y.; Chin, M. L. S.; Kudoh, S.; Takayanagi, M.; Nakata, M. Conformations of nitro-substituted spiropyran and merocyanine studied by low-temperature matrix-isolation infrared spectroscopy and density-functional-theory calculation. *Chem. Phys. Lett.* 2003, 370, 460-468.
- 46 Tomasi, J.; Cancès, E.; Pomelli, C. S.; Caricato, M.; Scalmani, G.; Frisch, M. J.; Cammi, R.; Basilevsky, M. V.; Chuev, G. N.; Mennucci, B. Modern Theories of Continuum Models. In *Continuum Solvation Models in Chemical Physics: From Theory to Applications*; Mennucci, B., Cammi, R., Eds.; John Wiley & Sons: Chichester, UK, 2007; pp 1–123
- 47 Wojtyk, J. T. C.; Wasey, A.; Kazmaier, P. M.; Hoz, S.; Buncel, E. Thermal reversion mechanism of n-functionalized merocyanines to spiropyrans: A solvatochromic, solvatokinetic, and semiempirical study. *J. Phys. Chem. A* 2000, 104, 9046–9055.
- 48 Castro, P. J.; Gómez, I.; Cossi, M.; Reguero, M. Computational Study of the Mechanism of the Photochemical and Thermal Ring-Opening/Closure Reactions and Solvent Dependence in Spirooxazines. *J. Phys. Chem. A* 2012, 116, 8148–8158.